International Hydrographic Review, Monaco, LVI (1), January 1979.

SEA BEAM, MULTI-BEAM ECHO-SOUNDING IN " JEAN CHARCOT "

DESCRIPTION, EVALUATION AND FIRST RESULTS

by Vincent RENARD
and Jean-Paul ALLENOU
Centre Océanologique de Bretagne, Brest

Contribution No. 301 of the " Département Scientifique ".

SUMMARY

In 1976, CNEXO (Centre National pour l'Exploitation des Océans) purchased a Sea Beam system, a 16-beam echo-sounder, from GIC (General Instrument Corporation), Harris A.S.W. Division, Westwood, Massachusetts.

This sounder was installed on the N.O. *Jean Charcot* and tested in the Spring of 1977. As opposed to a classical sounder which obtains only one bathymetric profile along a ship's track, this new type of sounder covers a swath of sea floor 3/4 the water depth wide (4 500 m for a 6 000 m depth) [1]. Bathymetric data are processed in real time by a mini-computer efficiently programmed to plot bathymetric contour lines at a contour interval and a scale set by the operator. Data are also recorded on magnetic tape for off-line processing.

The present paper presents the first results obtained with the Sea Beam during a 4-week evaluation cruise in April and May 1977, analyzed with the advantage of extensive further experience with the system. It explores also the potential of the Sea Beam for cartography and structural analysis.

INTRODUCTION

Systematic sounding of the deep sea floor started in the 1930's, when acoustic methods replaced the laborious use of the sounding lead. Although improved during and after World War II, acoustic sounding has not progressed significantly since and has remained limited to the measure of a single depth value at a time. This depth, measured at high repetition rates (2 seconds on the average), corresponds to the first echo received for most sounders in a non-stabilized cone of wide aperture (30 to 60 degrees) or, for some more sophisticated but far less numerous ones, in a cone of a few degrees stabilized for ship's roll and pitch in order to obtain the depth vertically below the ship. The accuracy of the depth measured depends on the aperture angle, and in deep water only narrow beam sounders can be used for precise mapping. Time required to complete a detailed survey is normally quite long, because several parallel lines set apart not more than the width of the ensonified area (a few hundred meters in deep water for narrow beam sonars) have to be run.

Only recently, a new step has been taken in the field of bathymetric sounding through the development of multi-beam echo sounders which provide at each ping not only the depth at the vertical beneath the ship but also several depth values transverse to the ship's track [2]. As the ship moves along, a swath of sea floor is swept with soundings over a width depending on the number of beams and their aperture. Depth values are digitized and plotted in real time as contour lines. Slopes and directions of sea floor relief are therefore immediately available to the party on board. Great progress in the study and understanding of sea floor morphology will be possible with this new generation of sounders. Time saving is propor-

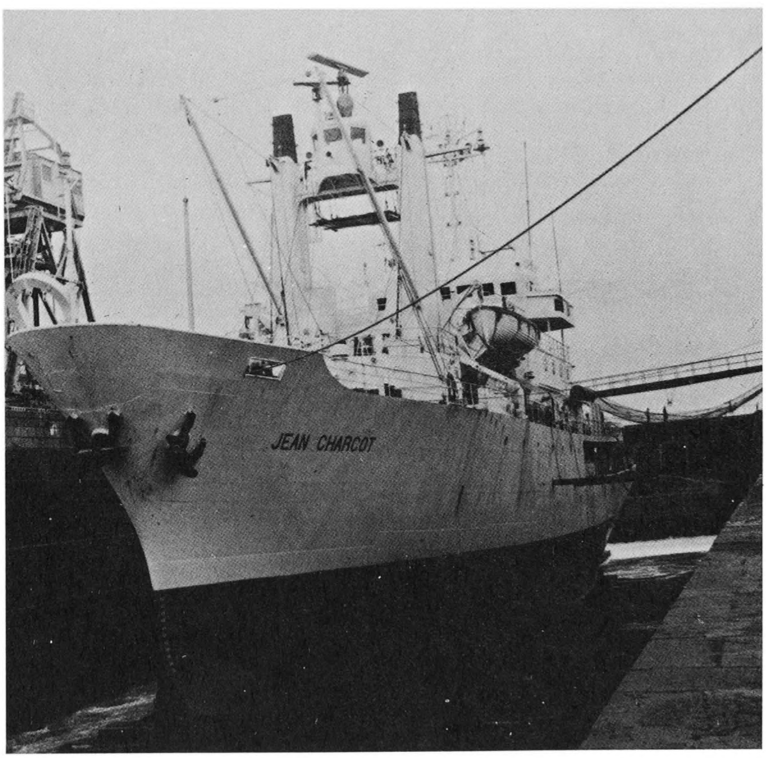

FIG. 1. — The N.O. *Jean Charcot* in dry dock during the installation of Sea Beam transducers, Brest, January 1977.

tional to the number and aperture of beams. The most recent of these developments is the Sea Beam, a system of 16 beams each of 2° 2/3 aperture, and for this equipment the time needed for a given survey is reduced by a factor of 10 or more over a mono-beam system.

Aware of the great advantages of this new tool for marine exploration, CNEXO has installed a multi-beam echo sounder on one of its vessels. Since May 1977, the N.O. *Jean Charcot* has been the first vessel in the world operating with a Sea Beam, manufactured by General Instrument Corporation (GIC) (fig. 1).

BEAM FORMING PRINCIPLE

Two groups of transducers are installed under the ship's hull, the projectors for acoustic signal emission and the hydrophones for reception of echoes from the sea floor.

Emission

The active part of the emission is made up of 20 projectors, each contained in a rectangular box (fig. 2). Each projector contains 4 magnetostrictive elements mounted in parallel. The 20 projectors are mounted in a 6 m long berth placed along the keel of the ship under a protective dome. Each projector is excited separately. By control of the power and phase of the emission frequency, the emission diagram shown in fig. 4 (A) is obtained. The area of sea floor ensonified after emission corresponds to a rectangular area subtending angles of 60° by 2° 2/3. The plane of emission is transverse to the ship and is electronically stabilized for ship's pitch (within 10°) so as to remain vertical.

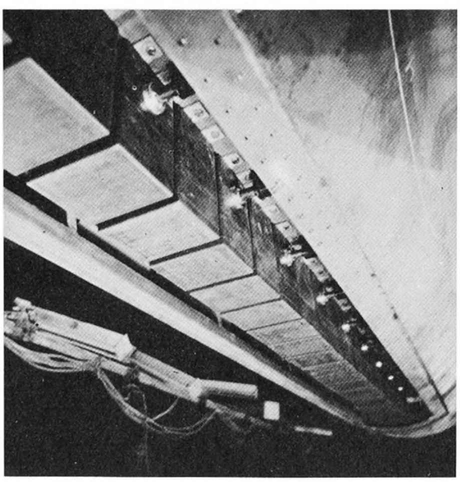

FIG. 2. — Sea Beam projectors during mounting under ship's hull.

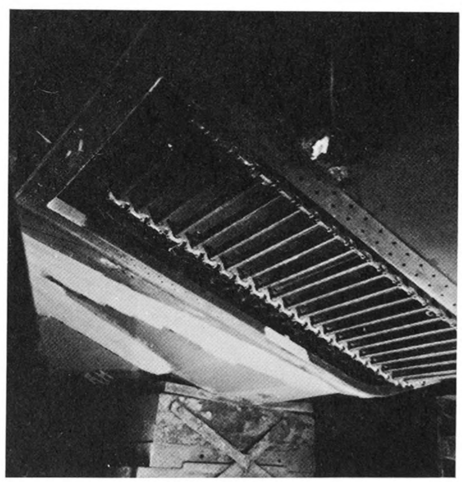

FIG. 3. — Sea Beam hydrophones during mounting under ship's hull.

Reception

Each reception hydrophone is made up of piezo-electric elements mounted with intercalating rings on a round bar covered by a rubber sleeve. The reception unit is composed of 40 such hydrophones mounted under a 4 m long protective cover transverse to the ship's keel (fig. 3). The 16 beams are obtained by vector summation of the signals received by these 40 hydrophones. Fig. 4 (B) illustrates the 16 beams so created.

They correspond to signals coming from 16 rectangular zones on the sea floor subtending angles of 20° by 2° 2/3 with the long side parallel to the ship's axis. These zones are not stabilized for roll or pitch.

Composite emission/reception

Fig. 4 C illustrates the creation of the 16 narrow beams as a result of the composition of the emission and reception diagrams of fig. 4 A and 4 B. The received acoustic energy comes from 16 " square " zones, 2° 2/3 by 2° 2/3, located in a vertical plane perpendicular to the axis of the ship, due to emission stabilization. Their transverse orientation varies continuously with ship's roll and is obtained by reference to a vertical gyroscope after reception of output signals.

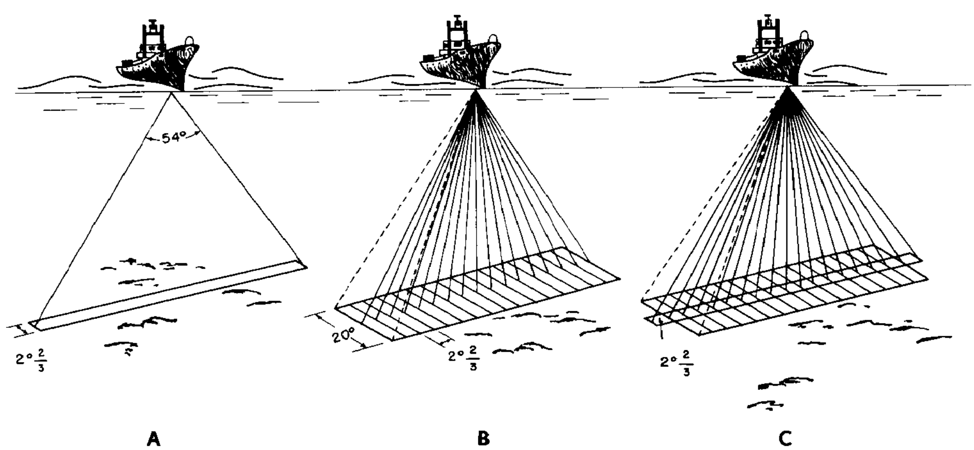

FIG. 4. — Beam forming scheme of the Sea Beam ; (A) zone ensonified at emission ; (B) zones covered at reception ; (C) zones resulting from the combination of A and B sounded by the multiple beams (usable ensonified area).

GENERAL STRUCTURE OF THE SEA BEAM

Details regarding the Sea Beam are given in a separate Technical Paper [3]. Only a general description of the Sea Beam's structure and outputs is given here.

The Sea Beam results from the integration of two systems. On the one hand, the NBES (narrow beam echo sounder) which yields only analog

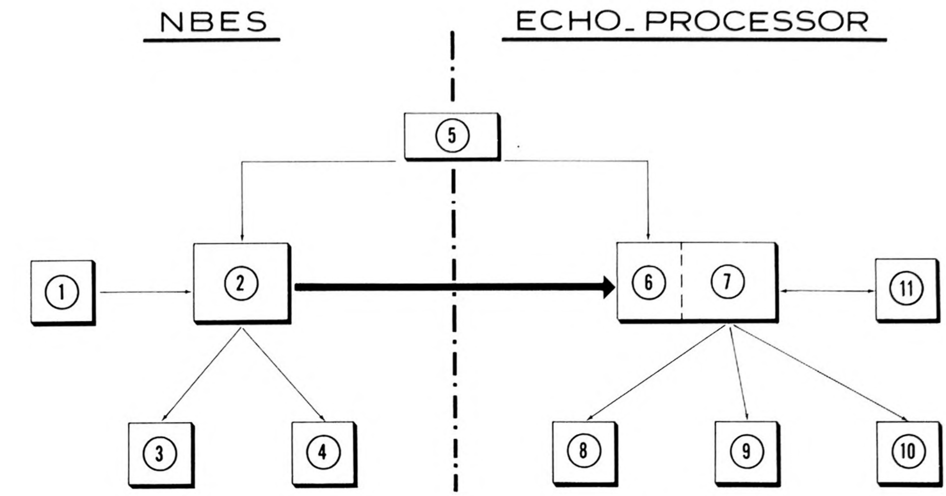

FIG. 5. — General structure of the Sea Beam, with on one side the NBES and on the other the Echo Processor : (1) transducers (projectors and hydrophones) ; (2) electronics of the NBES ; (3) graphic display of the vertical beam ; (4) digital display of the vertical beam ; (5) Vertical reference gyro ; (6) coupling between the NBES and computer ; (7) NOVA 800 mini-computer ; (8) CRT for transverse bathymetric profile ; (9) magnetic tape recorder for recording soundings and time ; (10) digital plotter for real-time contour line tracing ; (11) teletyper for system control.

Various components can be seen on fig. 6 and 7.

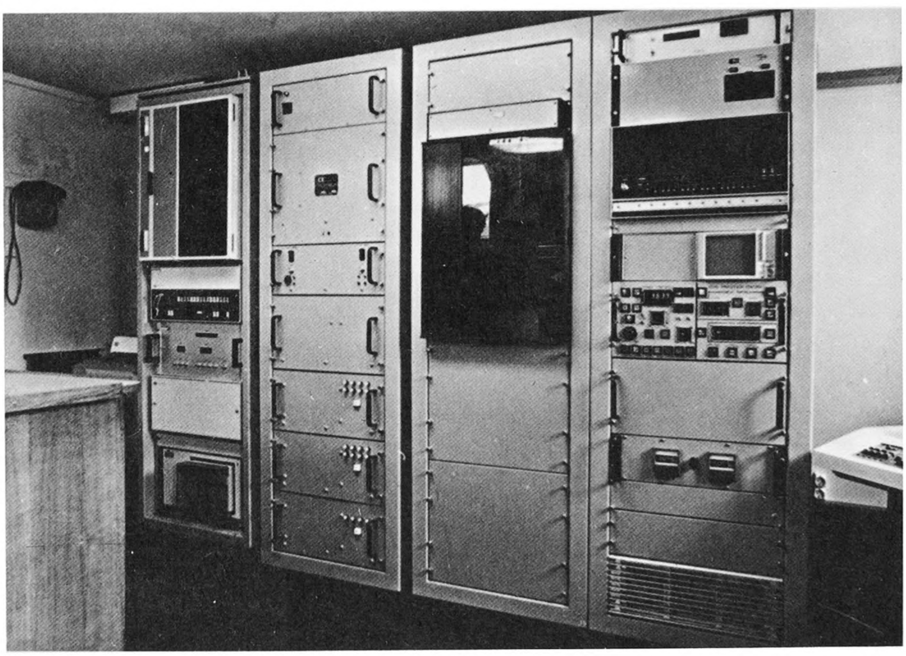

FIG. 6. — Sea Beam — General lay-out ; *left,* power electronics ; *centre,* magnetic recorder ; *right,* mini-computer, control panel, and CRT display.

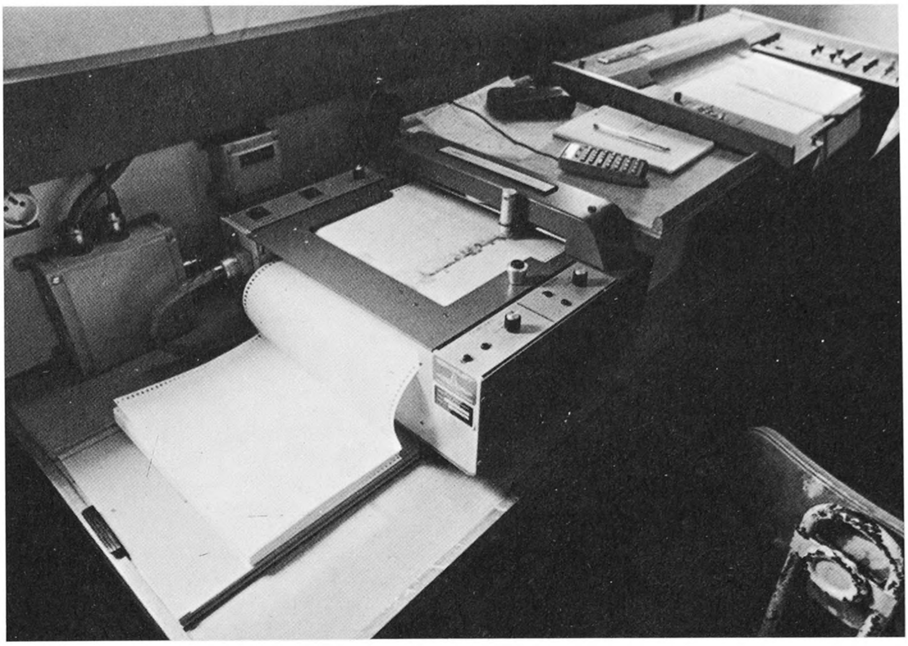

Fig. 7. — Contour line plotter and analog beam signal recorder UGR.

signals from the 16 acoustic beams, and on the other hand the Echo Processor which processes these signals through a mini-computer. Fig. 5 shows the general lay-out of the system which is installed in a special room on the ship (fig. 6 and 7).

NBES

The NBES functions are the following :

— power transducer excitation,
— hydrophone signal amplification,
— formation of 16 analog beams,
— hardware digitization of vertical beam,
— signal forming for processing and analog recording,
— hardware stabilization of roll.

The NBES operates in two main modes :

— Autonomous (group ping or periodic) : in this mode, the Echo Processor is disconnected and the NBES can be used as an analog narrow beam system. Group ping mode allows a high repetition rate with programming of emission and reception cycles via the graphic recorder UGR (Universal Graphic Recorder). A mean repetition rate of 2 seconds can be obtained for all depths using a 8-cycle program with a basic cycle time of one second. In the periodic mode, on the contrary, the NBES controls the emission as a function of a depth window chosen by the operator. Emission rate is determined by the time necessary for the sound to travel up to the deepest limit of the window.

— Under Echo Processor control : in this mode, the NBES is controlled by the mini-computer. Its role is identical but the cycle duration will be equal to the time needed for the echo to reach the ship plus a short processing time (less than one second). Fig. 8 illustrates a bathymetric profile obtained on the UGR in this mode. Total depth increment of the record is 750 meters, corresponding to the last second of reception. Depth can be obtained by interpolation between scale lines and addition of the number of 750 meter (one second) cycles corresponding to the number of seconds

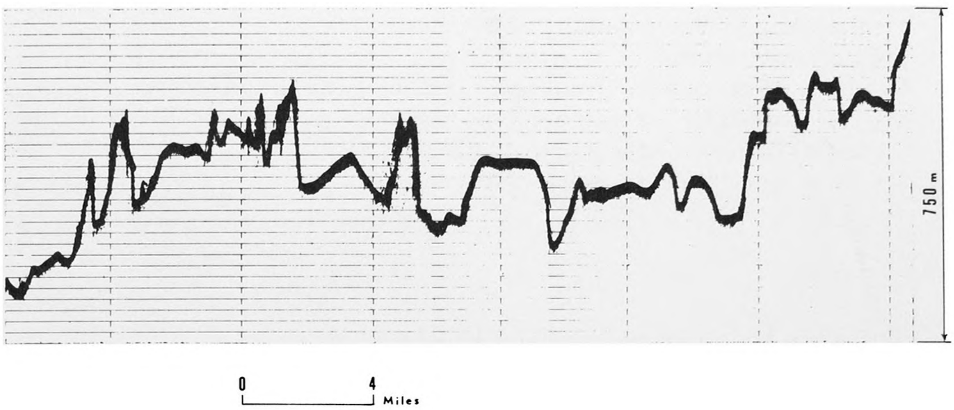

Fig. 8. — Example of analog vertical beam record in autonomous mode (repetition rate : 6 seconds).

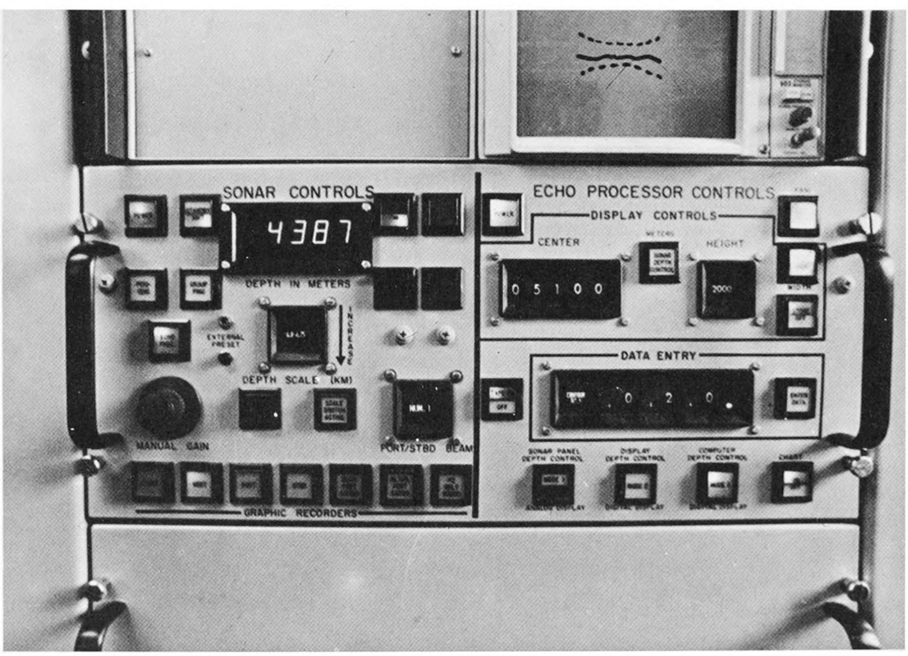

Fig. 9. — Control panel ; *left,* NBES controls ; *right,* Echo Processor controls ; in the *upper right* corner, display of the transverse bathymetric profile, reception gates appear as dashed lines.

elapsed before the one recorded. Oblique beams can also be displayed in analog form by selection on the NBES control panel (fig. 9), either each beam separately, all together, alternate port and starboard beams, or as port and starboard couples.

Depth of the vertical beam is also digitized by hardware (except in group ping mode) and displayed on nixie tubes on the NBES control panel (fig. 9) and repeated in the ship's scientific laboratory.

The left side of figure 9 represents the NBES control panel which includes :

— emission control, standby or transmit ;
— impulse duration, 1 or 7 msec ;
— mode of operation, group ping, periodic, or echo processor ;
— repetition rate in autonomous mode by setting a depth window ;
— depth display of the vertical beam ;
— beam selection for analog display.

Echo Processor

The main functions of the Echo Processor are :

— numerical processing of incoming signals from the hydrophones, calculation of depth and transverse distance to the ship for all beams ;
— magnetic tape digital recording ;
— digital plotter control ;
— CRT display of transverse bathymetric profile.

The Echo Processor operates under three different modes. In mode 1, unprocessed signals are displayed on the CRT in order to initialize various parameters and to control levels (noise, back-scattered energy, etc.). In mode 2, signal reception gates are controlled manually. In mode 3, gates are set automatically. Mode 3 is the normal mode of operation. Mode 2 is used for initialization or in case of signal loss.

Echo Processor controls are shown on figure 9 (right side) ; the upper part (display control) centers the profile on the CRT and selects the vertical exaggeration, the middle part (data entry) controls the entry of various parameters, mainly ship's speed and heading, plot scale and contour interval. In mode 2, the transverse bathymetric profile appears on the CRT for each ping linearly interpolated between the 16 beam values (fig. 9). The profile remains visible up to the next ping. In mode 3, reception gates are visible on both sides of the profile (fig. 9).

Two sets of data are recorded on magnetic tape to be used for later processing :

— Profile characteristics : cruise number, profile number, day of the year, comments ;
— Data for every ping : hour, minute, second ; heading, depth for each beam, transverse distance for each beam.

The digital plotter contours bathymetry along a rectified ship's track. Scale and contour interval are chosen by the operator. Slope is indicated by

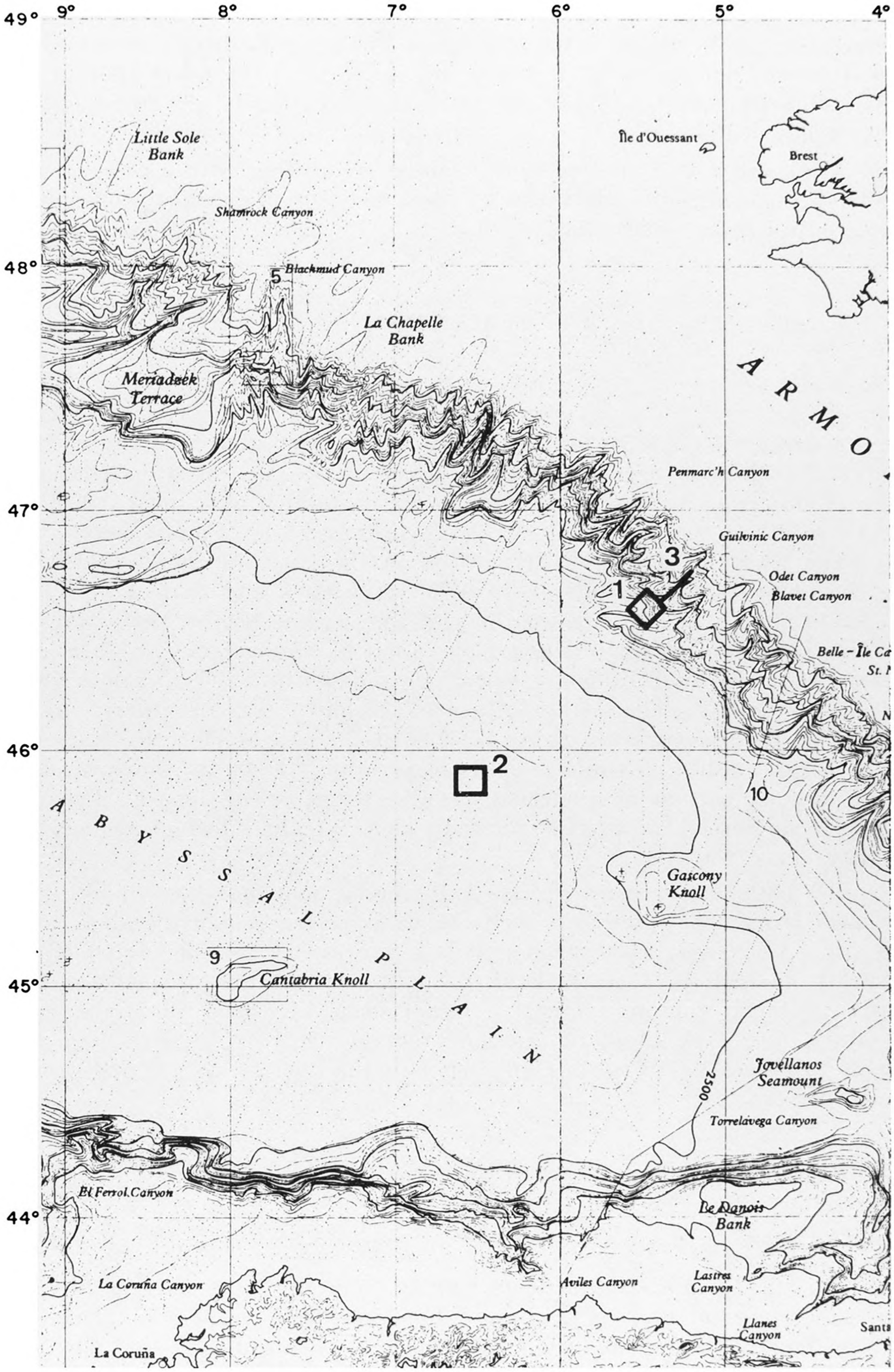

FIG. 10. — Test area locations on the Armorican continental margin off Brittany ; 1. slope area ; 2. flat area ; 3. Guilvinic canyon.

small marks bordering every other contour line and oriented towards increasing depth. Depth value of contour lines is periodically indicated by small marks across the central axis and written on the lower part of the plot. Hour, heading, and contour interval are periodically written on the upper part of the plot.

A telewriter is connected to the computer together with a cassette unit to load programs, initialize various parameters (sound velocity profile, etc.) and control system operation.

EVALUATION

Test zone

A test cruise (April 12 - May 18, 1977) has permitted the conduct of a detailed evaluation of the Sea Beam performance. In order to eliminate navigation errors, transponders for acoustic navigation were deployed in the test area. With such a system, navigation accuracy was of a few meters [4]. Test zones were located in the Bay of Biscay (fig. 10). One zone was selected in the abyssal plain (depth about 4 750 m, slopes less than 1/1 000) in order to check the ultimate accuracy of the various beams, their stability in time, and the various modes of operation of the system. Another zone was selected on the continental slope (depth 2 500 to 3 700 m, slopes 10 to 40 %) in order to check the influence of slopes and structures on the accuracy of the system. Because both zones had to be close to the ship's base, Brest, neither maximum depth of operation (12 000 m), nor operation over various bottom characteristics could therefore be tested. The test cruise time spread, however did permit checking the effect of various sea conditions on the system.

For both test areas, a precise bathymetric map has been made from vertical beam data alone in order to serve as reference. In the slope area, 32 track lines were run parallel with a spacing of 150 m controlled by acoustic navigation. Fig. 11 shows the bathymetric map obtained for that area (20 meter contour interval, original scale 1/10 000). It is the most accurate map that could be obtained for reference. A similar map was made to check the absence of any relief in the abyssal area which proved to be perfectly flat.

Qualitative analysis

Abyssal plain

Fig. 12 (A) and (B) illustrate results from the first tests in the flat area. Contour intervals of 2, 5 and 10 m have been selected in turn. One can estimate that the resolution of the system (all beams) at that time lay between 10 and 15 meters, since observed contours do not reflect sea floor topography, which is perfectly flat, but integrate several other effects. First of all, ship's heave, which is less than 2 m for the case shown. Secondly, the progressive decrease in accuracy the more oblique the beams

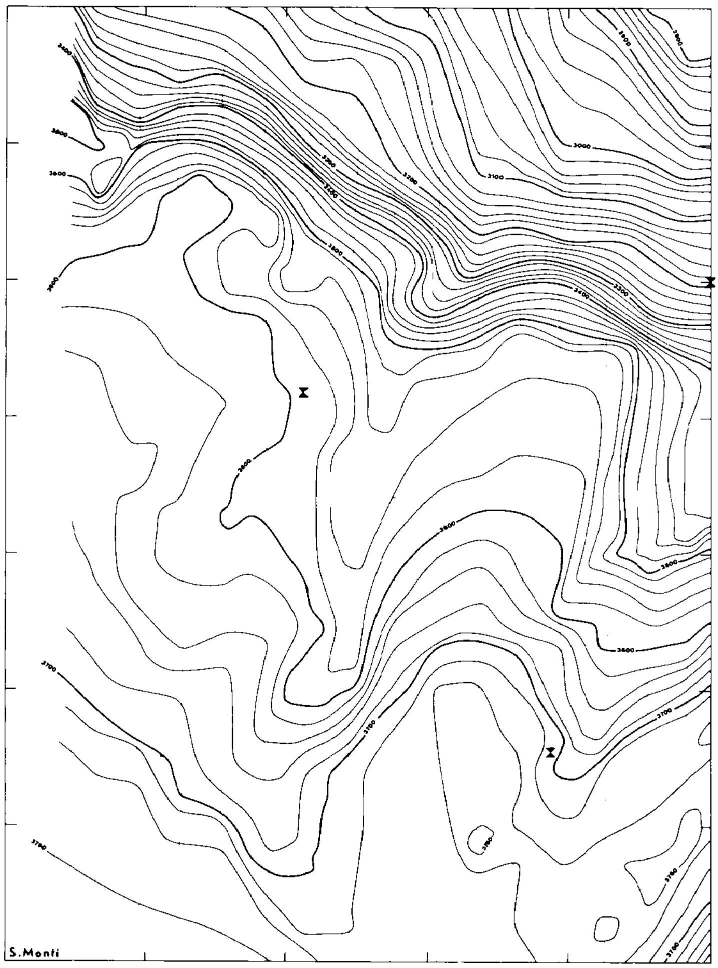

FIG. 11. — Bathymetric map of Test Area 1 obtained from vertical beam data only and 150 m track line spacing with acoustic navigation (only every other line shown). Frame marks spaced at 1 000 m.

are to the ship's axis. Thirdly, some systematic errors, such as the deeper zone below the median line of fig. 12 A which always appeared on the starboard side whatever the ship's heading. The source of these errors is discussed later and solutions have been found to reduce their effect.

Slope area

In order to compare Sea Beam plots to the reference map (fig. 11), the following assemblages have been made. Sea Beam plots, such as fig. 13, have been cut along their median line and one half has been aligned along the corresponding ship track by matching time marks. Exact alignment could only be obtained for one time mark because the speed used for the Sea Beam plot did not correspond exactly to ground speed. Away from this match point, shifts appear in the alignment of the contour lines from profile to profile which reflect errors that are more navigational than

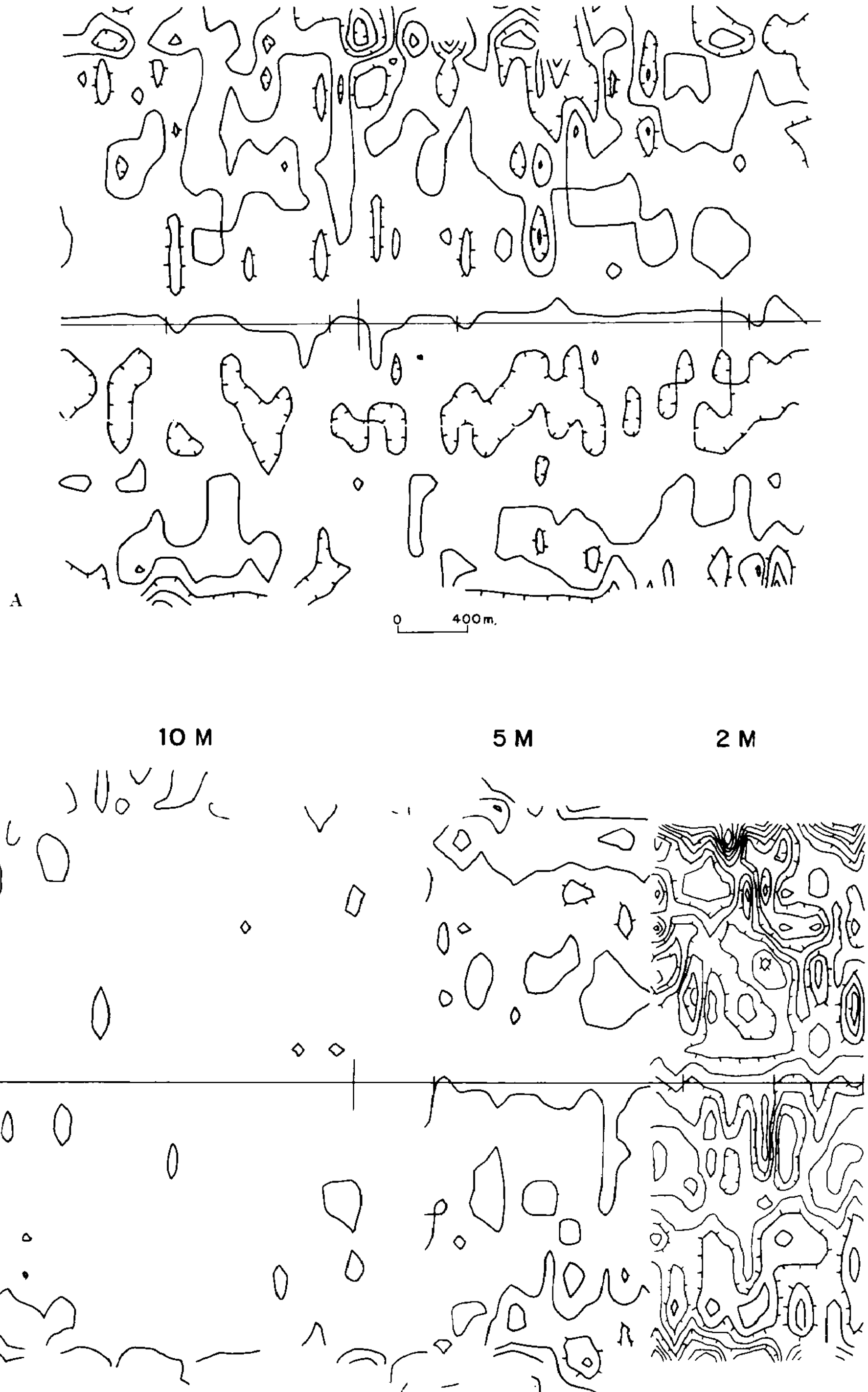

FIG. 12. — Figure drawn from real time contour line plot in the Bay of Biscay abyssal plain (Test Area 2) with various contour intervals ; (A) 5 m ; (B) 2 m, 5 m, and 10 m ; original scale 1/20 000.

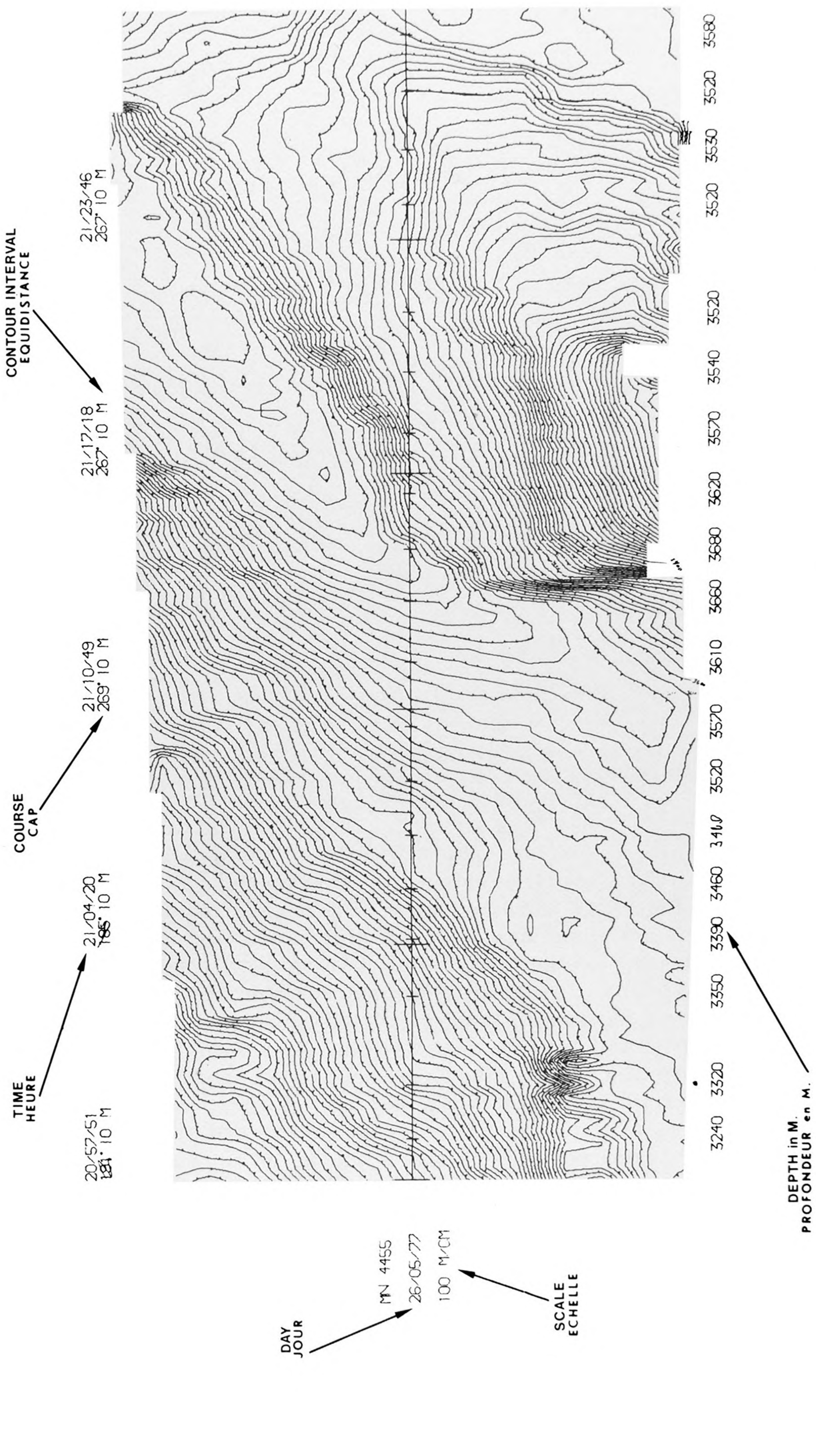

FIG. 13. — Real time plot from the Armorican continental slope off Brittany, contour interval 10 m, original scale 1/10 000.

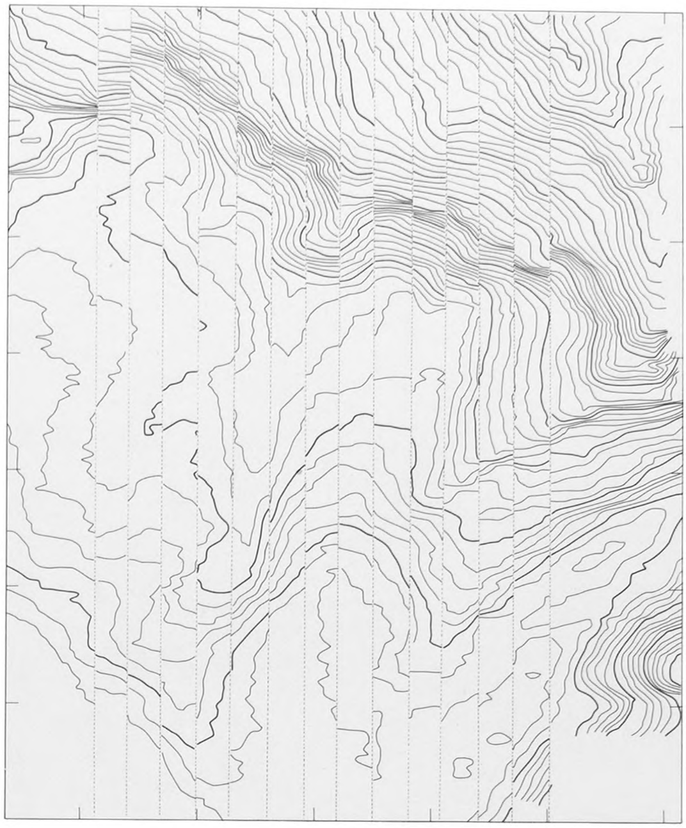

FIG. 14. — Slope area (Test Area 1). Map made from halves of Sea Beam plots for N-S tracks at 300 m spacing tied with navigation plot at mid-point of profiles.

bathymetric. These assemblages are therefore of qualitative value only. Figure 14 shows the assemblage obtained by overlapping plots with 300 m track spacing. Figure 15 shows a similar assemblage for 1 200 m track spacing. This figure illustrates well the progressive decrease of swath width with decreasing depth. Comparison of these two figures with figure 11 shows several points. First of all, if the map constructed with the vertical beam alone is more pleasing to the eye, it has become so in part by eliminating minor structural features such as local slope variations along the WNW-ESE escarpment. These minor features are not artifacts as they are repeated from profile to profile, and they are of some interest for the structural analysis of the area. Secondly, the decrease in accuracy as the obliquity of the beams increases is rather minor, as shown by the good match of the vertical beam data where it overlaps different oblique beams in both figures. The total swath is therefore mapped with almost even accuracy and a great overlap is not necessary. This slow degradation of the accuracy with obliquity is remarkable and is a major asset of the system. Thirdly, time reduction in ship time needed to conduct a survey is function of the overlap between lines but should be greater than a factor of 10 in almost any case. Fourthly, the need for the best estimate of ground speed is well illustrated by the increasing misalignment of contour lines away from the center of the zone. Finally, a later comparison made of figures 14 and 15 with E-W lines crossing the N-S network showed that the accuracy is independent of ship's heading for all practical purposes.

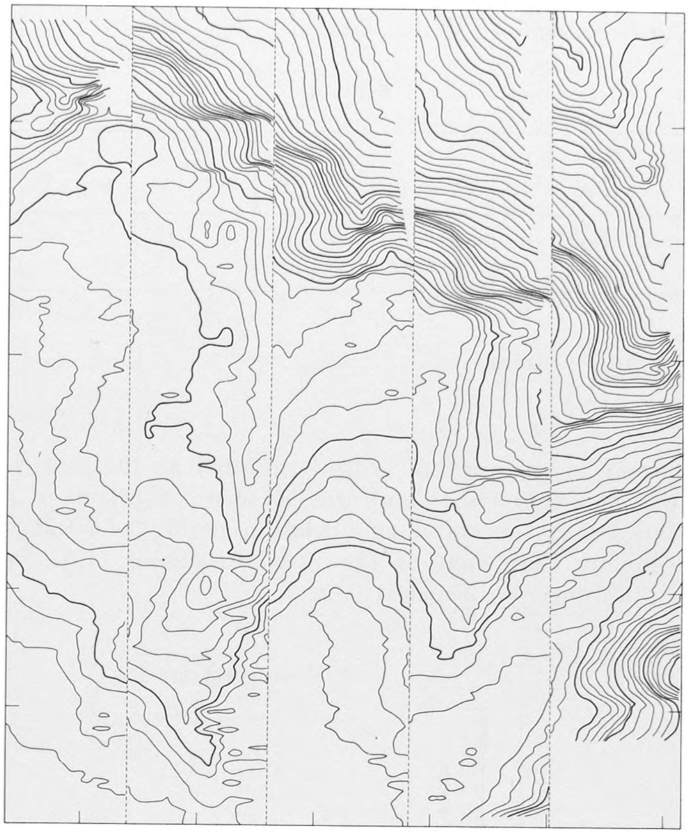

FIG. 15. — Slope area (Test Area 1). Map made from halves of Sea Beam plots for N-S tracks at 1 200 m track spacing tied with navigation plot at mid-point of profiles.

Quantitative analysis

Flat area — NBES

VERTICAL BEAM

The accuracy of the vertical beam has been measured over two hour periods. Comparison between the depth measured from the graphic recorder and the depth given by the NBES digitizer gives 0.2 meter rms error. Stability has been measured by comparing series of measurements spaced in time. Observations made over several days have shown fluctuations of 4 meters' amplitude with a tidal period which could be correlated with data from the tide gauge at La Rochelle. After correction for this tidal effect, standard deviation from one set of measurements to the other has been found to be of the order of 0.65 meter in the 4 750 meter water depth of the test area.

OBLIQUE BEAMS

Comparison between the vertical beam and discrete values measured on the graphic recorder switched in turn from one beam to the next, gives the differences in Table 1. These differences are larger than those obtained with the Echo Processor, as shown later.

Table 1

Beam	2 P	2 S	3 P	3 S	4 P	4 S	5 P	5 S	6 P	6 S	7 P	7 S
Difference (m)	0	9	–3	–1	–6	15	–7	10	–9	16	–16	–7

Flat area - Echo Processor

VERTICAL BEAM

The accuracy of the vertical beam computed as the rms value of the differences between the NBES and the software digitizer is 1.62 meter. Figure 16 shows that the standard deviation from the NBES digitizer is smaller (0.4 meter) than that of the Echo Processor (1.67 meter). The cause of this difference is discussed later.

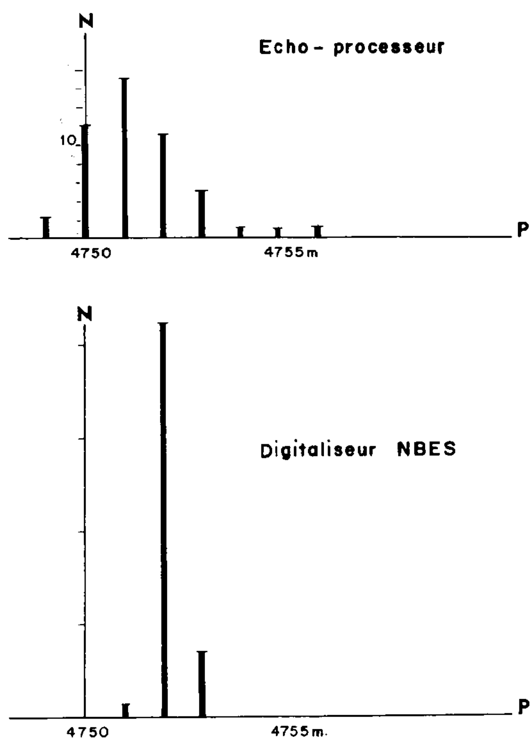

FIG. 16. — NBES and Echo Processor vertical beam digitization ; histogram of number of interrogations versus depth.

Oblique Beams

A special program has been used to measure statistically the accuracy of the oblique beams. The program gives the mean and the rms value of the difference between each oblique beam and the vertical beam taken as reference for 400 cycles. Results are shown in table 2 and plotted in figures 17 A and B. Figure 17 A shows that the rms value varies little from beam to beam. Values obtained for the most oblique beams are small. For beam 6, for example, one can compute that the observed error corresponds to an angular offset of a quarter of a degree. Beams close to the vertical (1, 2, 3) however are not as accurate as expected. Figure 17 (B) gives the mean difference of the systematic error between each beam and the vertical

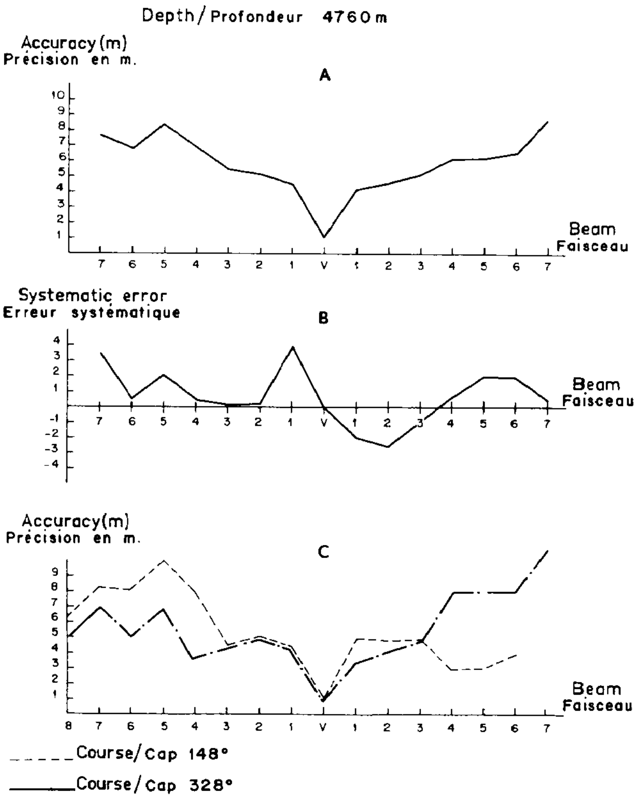

Fig. 17. — Accuracy test in flat area ; (A) RMS values for each beam ; (B) systematic error for each beam ; (C) RMS as a function of course.

Table 2

Beam	1 P	1 S	2 P	2 S	3 P	3 S	4 P	4 S	5 P	5 S	6 P	6 S	7 P	7 S
Mean difference	4.0	−2.0	0.0	−2.5	0.0	−1.0	0.5	0.5	2.0	2.0	0.5	2.0	3.5	0.5
R M S	4.5	4.2	5.1	4.6	5.5	5.2	6.9	6.2	8.4	6.1	6.8	6.6	7.7	8.4

one. These errors are small except for port beam 1 (4 meters) and starboard beams 1 and 2. A systematic correction has been introduced to cancel these offsets until their cause is better understood. Figure 17 (C) illustrates a curious phenomenon observed in the flat area. The same track has been sailed twice on opposite courses. RMS values for the central beams vary little, but for oblique beams the largest rms values change from port to starboard as the ship reverses course. This course is parallel to the lower continental slope and the observed reversal could be due to the structure of surficial sediments or ripple marks. Indeed a large variation (— 10 dB) in the level of backscattered energy has been measured with the change in ship's heading.

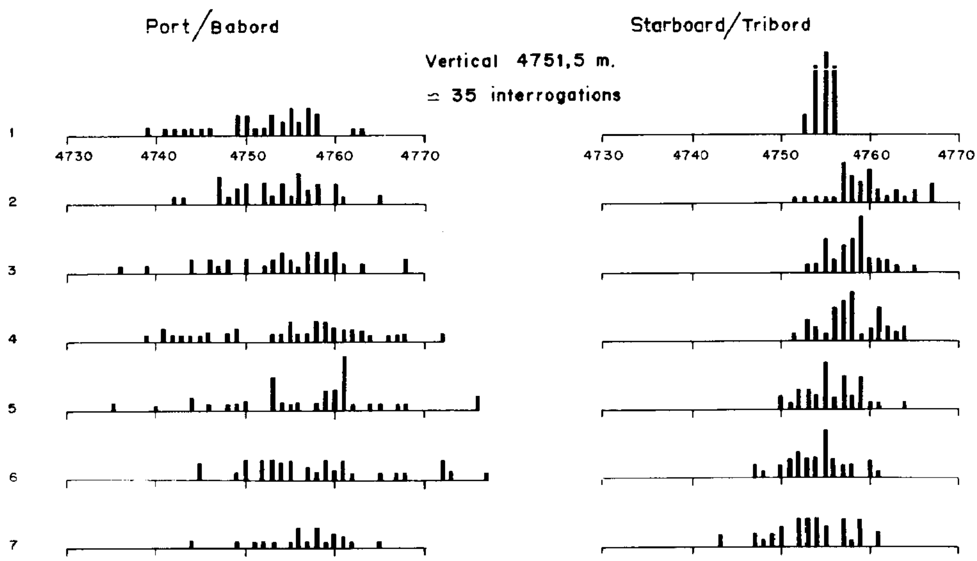

FIG. 18. — Depth dispersion over flat area for each beam, and for 35 individual pings.

Figure 18 shows the distribution of 35 discrete pings at ship's heading of 148°. The asymmetry in port and starboard values is well displayed. This figure also shows that if only discrete values were used, differences of + or — 10 meters can be observed even for near-vertical beams. Quite clearly, processing of a great number of values by the Echo Processor yields statistical estimates of the real depth and significantly increases the accuracy of the system. For that reason, if the greatest accuracy is desired ship's speed should be reduced, especially over strong slopes. Figure 12 illustrates the effect of these variations on Sea Beam plots. The greater variance of port beams at course 148° generates a noisier plot. The elevated area seen on the port side of the track and the small depression on the starboard side reflect the systematic errors on those beams as shown on fig. 17 (B).

Inclination

In order to verify the good stabilization of the system a 5° list was given to the ship with ballast. Rms values are given in table 3. Two extra beams on the port side (Nos. 8 & 9) have replaced two starboard ones. Values are very close to previous ones and no error in stabilization seems to exist.

Table 3

Beam	1 P	1 S	2 P	2 S	3 P	3 S	4 P	4 S	5 P	5 S	6 P	6 S	7 P	7 S	8 P	8 S	9 P	9 S
RMS	3.2	6.7	7.8	5.0	8.1	6.0	6.1	6.4	5.9	7.1	7.3	7.1	6.1	...	7.5	...	10.7	...

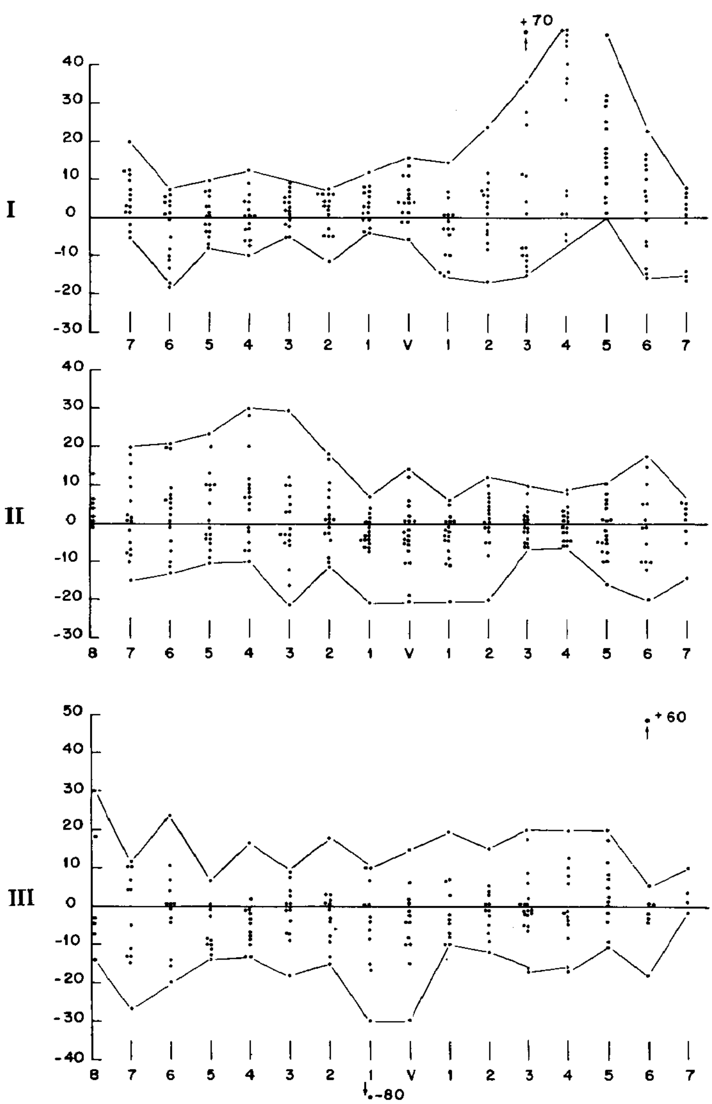

FIG. 19. — Slope area : difference (in meters) between oblique beam and vertical beam as reference for three profiles I, II and III. Dots represent data points taken along ship's track.

Slope area

Four lines (2 N-S and 2 E-W, 1 000 meters apart) run with acoustic navigation have been used for comparison with the vertical beam reference map. Differences between oblique and vertical beams measured on the map are presented in figure 19 for three profiles. Corresponding rms values are given in figure 20. Mean slope for these profiles was 10 % with local

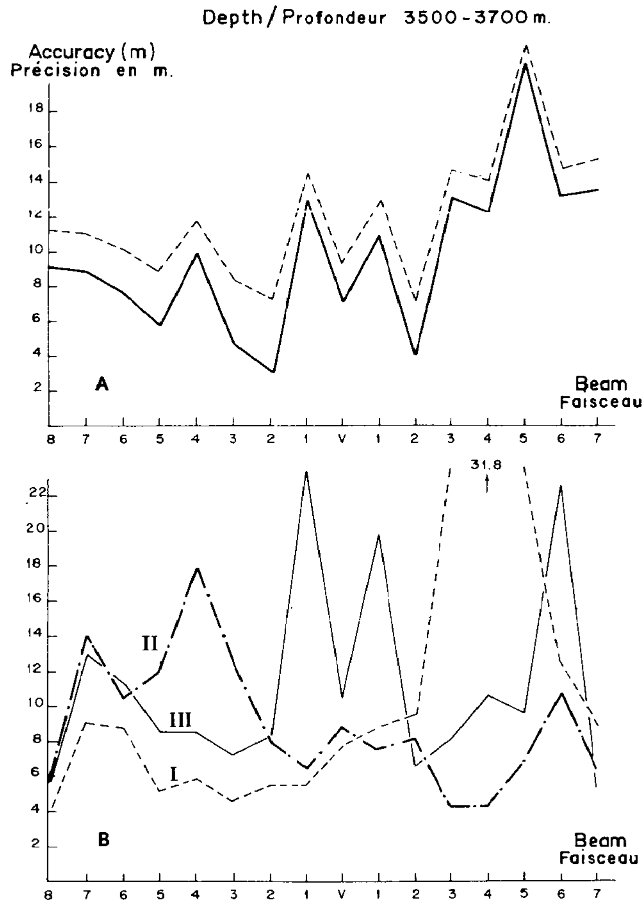

FIG. 20. — Slope area : (A) RMS value for each beam corrected for vertical beam variance for profiles I, II and III combined ; (B) RMS value for each profile separately.

maxima of 40 %. The mean accuracy for all beams is of the order of 10 to 15 meters but its distribution is less homogeneous than in the flat area. On line I, starboard beams give large discrepancies. A closer look reveals that these result from particular sea floor morphology. Seven individual cycles have been closely examined and results are given in table 4. This table gives the difference between the vertical and each oblique beam measured on the maps, as well as slopes given by Sea Beam plots. Although the largest discrepancies coincide with the steepest slopes, discrepancies remain larger than on lines II or III, especially for Beam 4 with a high rms value of 28 m. The largest differences occur on top of a N-S rounded

Table 4

Interrogations	Difference between map and Sea Beam values							
	Port beam number							
	1	2	3	4	5	6	7	8
1	7 % − 1	20 % + 14	5 % − 2	10 % − 20	15 % + 4	10 % 21	10 % 2	10 % 9
2	+ 1	+ 15	1	10 % − 19	18 % + 15	10 % 9	20 % 3	15 % 8
3	+ 5	+ 2	− 1	12 % + 47	+ 12	6	− 6	− 7
4	− 4	− 12	23	40 % + 31	+ 24	17	− 7	− 10
5	− 6	+ 5	16	10 % + 3	+ 6	11	− 16	3
6	9	10	16	8 % + 5	+ 2	1	− 5	0
7	0	− 15	0	40 % + 42	+ 37	5	− 17	−

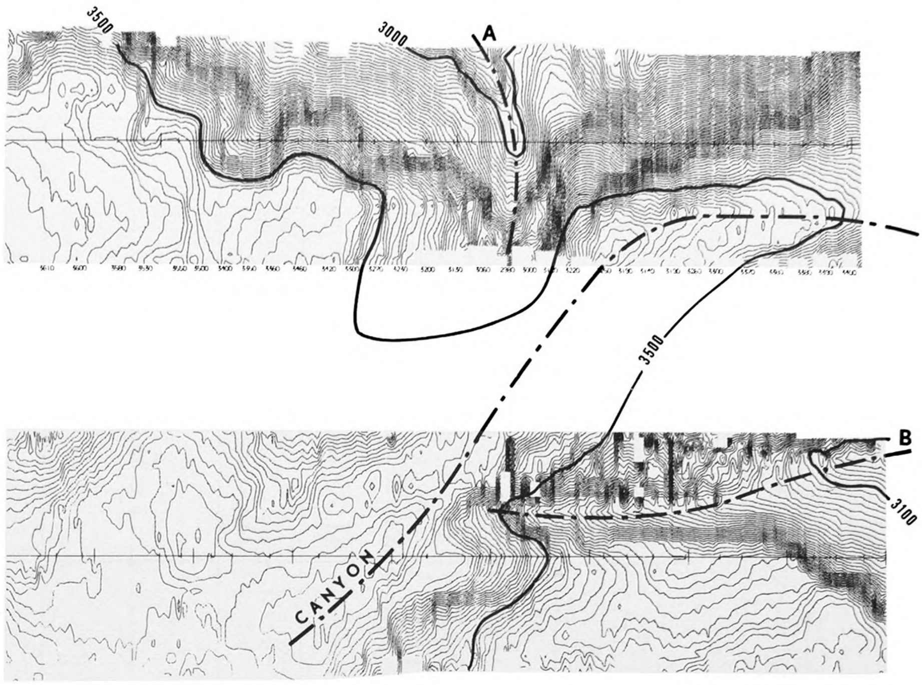

FIG. 21. — Contour plots for two parallel lines intersecting a canyon. The presence of ridge B creates errors on the lower line beyond that ridge.

topographic high. This particular morphology is such that arrival times of beams 1 to 4 are almost synchronous. Furthermore, due to the slope, mirror reflection lies close to beam 4. It appears that the system could not differentiate this high energy reflection coming through side lobes from the synchronous low level backscattered energy entering the main lobe of beam 4. A similar case was found later during the tests, and is shown in figure 21. Two parallel lines intersect a canyon some distance apart. On the upper line no anomalies can be seen in the contour lines, even with slopes exceeding 100 %. On the lower line however, the presence of ridge B parallel to the course of the ship creates noise in the contour lines beyond the ridge. A close analysis shows that the ridge advances the oblique beams in time until they lead the vertical beam, then slows them down until they lag it. This overlap in reception time is such that the system will again be unable to reject high energy side lobe signals, especially because backscattered energy from the slope beyond the ridge will be even weaker than normal. This situation, however, is not very frequent because it requires a rare geometry.

Miscellaneous

Comparison with wide angle sonar

Figure 22 illustrates the bathymetric profile obtained along the lower line of figure 21 with a wide angle single beam sonar. The passage of the transverse canyon shows so much loss that its direction cannot be guessed

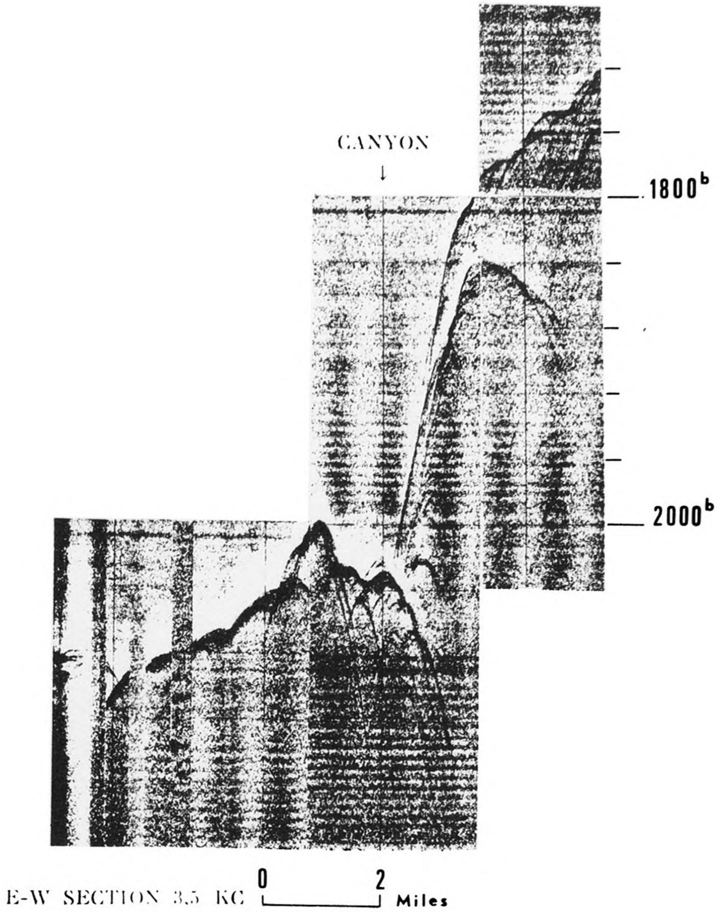

FIG. 22. — Wide angle echo sounder profile along lower line of fig. 21.

from that record. Slopes are greatly attenuated and the presence of multiple side echoes does not permit one to determine the depth vertically beneath the ship. The comparison of figures 21 and 22 illustrates better than all else the great advance of multi-beam techniques over existing monobeam systems.

Shallow water

Although the Sea-Beam is not adapted for shallow water, tests have been made over the continental shelf and in the Ushant Trough. Two situations seem to occur :

1. When the reverberation coefficient of the bottom is high relative to reflection, an accuracy of 0.5 m rms can be obtained as shown by figure 23 for one crossing of Ushant Trough (one meter contour interval).

2. When reverberation is too small relative to reflection, side lobe rejection becomes difficult and the accuracy drops down to 2 to 3 meters rms, which is not sufficient for detailed shelf surveys. This low accuracy

comes from the too-long emission pulse and the too-long sampling interval (3.3 m sec) used to digitize the received echoes.

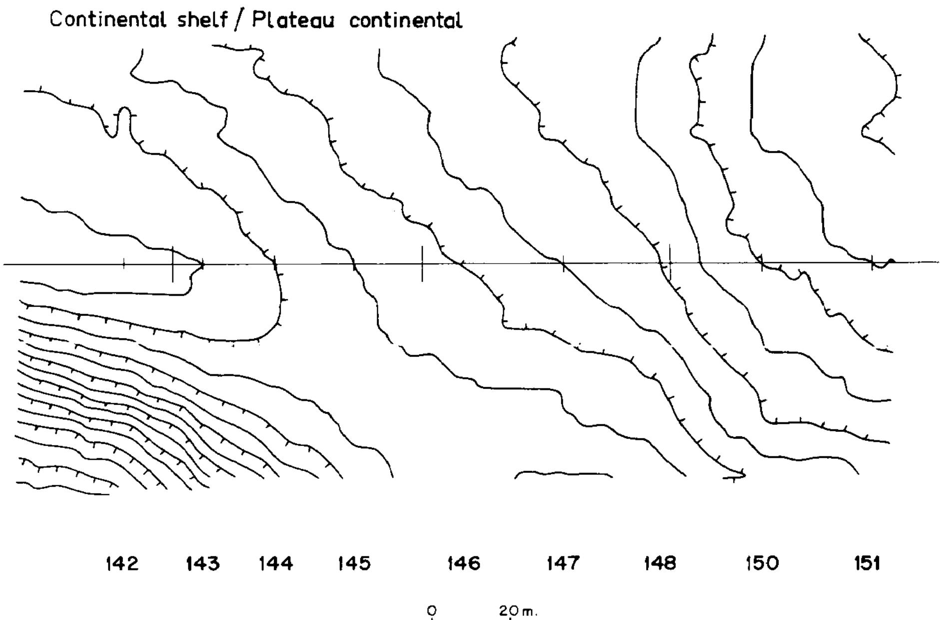

FIG. 23. — Figure drawn from real time contour line plot from the continental shelf, Ushant Trough, 1 m contour interval, scale of the original record 1/1 000.

Furthermore in shallow water, the width of sea floor band covered by the Sea Beam becomes small, and very accurate navigation is needed. The Bo'sun, developed also by GIC, is a multi-beam system better adapted to shallow water work [5], [6].

Speed influence

Tests of speed influence over Sea Beam performance have been run, from stop to full ahead (13.8 knots). No influence of speed on the quality of the results could be detected in the flat area. Table 5 gives the rms values for 13.3 knots. The increase in hydrodynamic noise stays limited relative to ambient noise. With the exception of steep slopes, the loss of data density versus distance for a given emission cycle due to increased speed does not cause a loss in quality of contour lines. Data density along the ship's track will always remain higher than lateral density even at maximum speed, and a smoothing of data will always take place.

Table 5

Beam	1		2		3		4		5		6		7		8	
	P	S	P	S	P	S	P	S	P	S	P	S	P	S	P	S
R M S	4.5	5.4	7.1	4.1	5.4	5.1	5.0	5.1	5.0	8.9	6.3	7.1	6.3	9.1	7.1	8.6

Sea state influence

Sea state is a determining factor in the good operation of the Sea Beam. The most critical point is the occurrence of air bubbles masking projectors and hydrophones. The situation appears when the ship pitches heavily at sea state 5 if sailing head on into the waves at full speed, or sea state 7 if sailing away. Degradation of record quality is progressive but the system will still operate. Speed reduction will allow work in higher sea states.

Maximum depth

At the time of this article, maximum depth encountered has been 7600 meters in the Romanche Fracture Zone. No loss of data has occurred. Maximum depth, as given by the manufacturers, is 12 000 meters.

TECHNICAL RESULTS

Transducer directivity

Emission

Measurements have been taken as follows : a hydrophone, positioned by a relay transponder over an array of bottom transponders [2], is lowered to the required depth by means of a conducting cable. The ship is manœuvred in order to swing the hydrophone along a segment of circle in the vertical plane longitudinal to the ship. The received signal is amplified and transmitted to the ship. Figure 24 shows the resulting emission diagram. Main lobe directivity measured at 3 dB attenuation is 2.9° against 2.66° announced by the manufacturers. The difference is small, and could be due to the method used. Secondary lobes are 4 to 5 dB higher than announced. At 4°, 8° and 22°, 23 dB attenuation is observed. The mirror lobe at 54° to 58° has a low 10 dB attenuation.

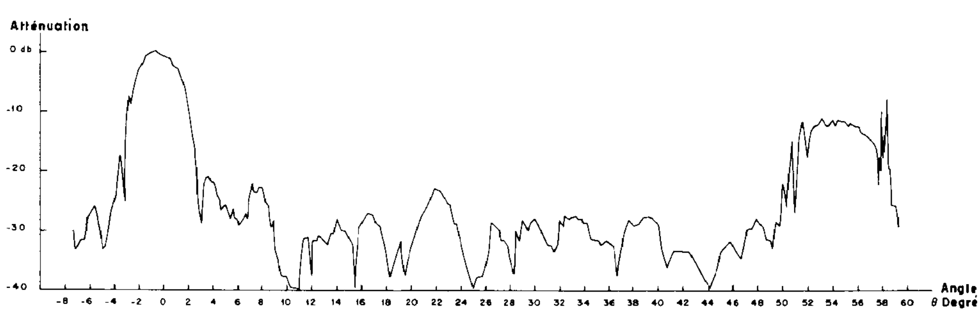

FIG. 24. — Emission diagram of Sea Beam : attenuation versus angle.

Reception

Measurements have been taken by lowering down to a depth of 2 000 meters a pinger tuned to the exact frequency of the Sea Beam (12 157 cps).

The pinger was positioned by a relay transponder via three bottom transponders. The ship was manœuvred laterally so the pinger would describe an arc of circle in the plane transverse to the ship for its emission to intersect each receiving beam. Because of ship's roll measurements have been

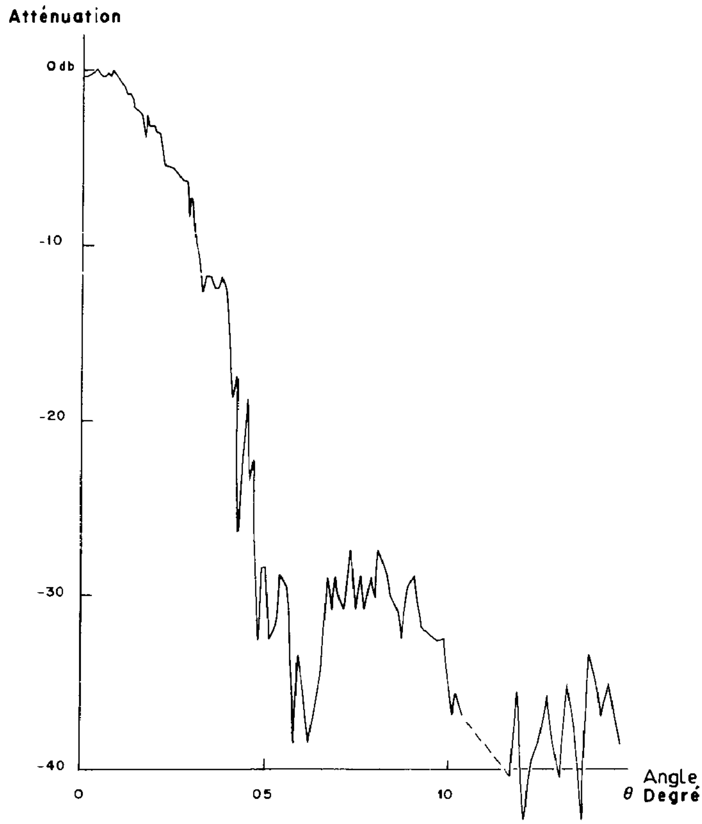

FIG. 25. — Vertical beam reception diagram : attenuation versus angle.

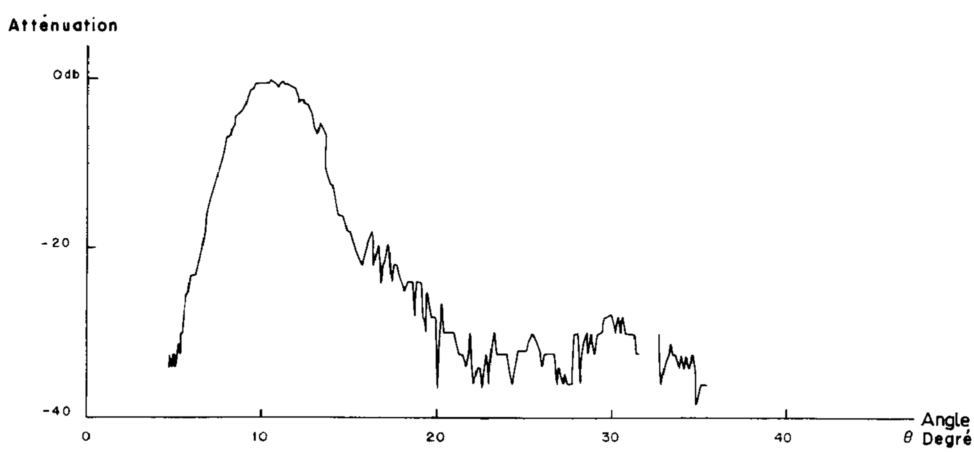

FIG. 26. — Beam No. 4 reception diagram : attenuation versus angle.

taken after stabilization. Figure 25 shows the reception diagram for the vertical beam. Directivity is 3.4° and side lobes are attenuated at 28 dB. Only one oblique beam (No. 4) has been measured and the resulting diagram is given in figure 26. Directivity is 3.4°. The main lobe seems to be asymmetric probably due to the V shape of the reception transducers (fig. 3). Secondary lobes are well attenuated.

Emission level

Emission level was found to be 130.1 dB at one meter.

SYSTEM EVALUATION

Although our tests have fully confirmed the validity of the system, a few remarks can be made.

Hardware

Figure 16 shows the superiority of the hardware digitizer over the software one. A certain improvement should therefore be possible as far as dynamic range and digitizing interval are concerned.

Dynamic range

The A/D converter has to be placed in the best condition of operation, and this is done by the TVG (time variable gain). The gain has to be high enough to digitize with accuracy the low level backscattered energy, but not too high in order not to saturate with the high level specular energy. The present dynamic range of 72 dB seems insufficient ; the necessity to avoid saturation results in a loss of accuracy in the digitization of the reverberated energy. This point seems to be the most critical of the system.

Digitizing step

Each channel is digitized with a 3.3 msec interval. This seems a little too long and results in generation of 1 to 2 meters noise (fig. 16).

Software

The heart of the Sea Beam is its software which processes signals from the NBES. One of the most delicate problems seems to be side lobe rejection because the specular energy is always very high compared to the backscattered one. For a given beam, the method used seems to work when the two energies are well separated in time. Otherwise, either in shallow water or for special bottom configuration as shown in table 4 and figure 21, separation is improperly done and yields large errors.

Outputs

The Sea Beam digital plotter contours are of the greatest value. It is fascinating to see the sea bottom structures being drawn under your eyes in real time as the ship moves over them. Two improvements should increase the contours' value even more. First of all, in the early version ship's speed was introduced manually, and only reflected a mean speed given by the ship's navigator. Direct coupling to the ship's log would have permitted one to integrate minute variations of speed. This coupling was implemented in June 1978 and has proved very satisfactory.

For the time being, whenever necessary to palliate the lack of precise navigation, a small overlap between lines and a few cross lines have been sufficient to assemble bathymetric maps from the real time plots without any major problems [7]. Positioning error due to the use of a speed different from true ground speed results in a longitudinal distortion of contour lines. This deformation has never been important enough to prevent matching overlapping lines. A complete integration of the Sea Beam data with navigation would be the second improvement, and a highly desirable one. This integration would provide contour lines directly in geographic coordinates. It would also take into account ship's yaw and drift. It would permit work at any scale without loss of accuracy due to contouring. In the present method of contouring, a fixed grid space is used. The number of data averaged over each grid cell will therefore vary with the ship's speed and the plot scale. This in turn forces the user to choose the largest possible scale in order to limit data smoothing. A grid space varying with the scale chosen would insure more flexibility and constancy of contouring characteristics.

In order to prepare this integration, software has been developed at CNEXO. This software processes the data recorded on magnetic tapes. It merges Sea Beam with navigation data and contours bathymetry in geographic coordinates. Transfer of this software to the ship is highly desirable, as soon as it is fully operational.

A solution to integrate, in real time, Sea Beam data with satellite navigation coupled with a doppler sonar or an inertial platform and predictive filtering is under study, and should improve the match between overlapping lines for ocean navigation [8], [9].

SEA BEAM USE

The Sea Beam opens up new horizons in the field of bathymetry for scientific and applied research, as well as in the realm of systematic marine cartography.

The main advantage over mono-beam techniques is that it provides 16 equivalent mono-beam tracks without the absolute need for precise ship positioning that would exist in order to get an equivalent set of data with a mono-beam system. Further, with required mono-beam track spacing

FIG. 27. — Bathymetric map assembled from Sea Beam plots and Decca navigation. Test Area 1 is outlined. Frame marks spaced at one minute of latitude or longitude, contour interval 20 m.

varying from 10 m on the shelf to 300 m in the deep ocean, the time necessary is so large that very few detailed surveys of the sort have been conducted up to now [10]. With the Sea Beam such detailed work will be done routinely.

Isolated track line

Sea Beam data collected along isolated lines have proved to be highly profitable. Systematic reading of sea floor structure orientation permits one to reveal the tectonic style of the area and to correlate it, for example, to an oceanic or a continental origin. Single tracks have shown up the existence of volcanic vents along mid-ocean ridges, or the sinuous course of a submarine canyon, etc.

Exploratory surveys

The Sea Beam is a tool well suited for exploration. It permits one to explore new study areas rapidly without the need for full bathymetric coverage. As an example, at the end of the Sea Beam tests, a few lines have outlined the structure of the continental margin around Test Area 1 (fig. 27) [11]. As part of this survey most of a canyon's meanders were sailed over, with the Sea Beam as a guide. Knowledge of the trend and slopes of this canyon will permit more detailed studies, such as dredging, coring or diving.

Detailed cartographic coverage

Figures 14 and 15 illustrate the use of Sea Beam for detailed mapping utilizing a highly precise navigation system. However, as one moves away from shore, navigation accuracy usually decreases. To counteract this, as water depth increases, the width of the Sea Beam bands increases and so does the possibility of localizing large typical structures such as scarps and seamounts, which may be used as a tie point in a survey. Several local surveys have been made with dead reckoning alone, using such tie points for the mosaic mounting of Sea Beam contours. In the absence of any characteristic seafloor feature the assemblage will become more difficult, and even become impossible in flat areas but there the need for precise mapping is less acute.

Station work

For station work one usually wishes to keep the ship fixed relative to a sea floor structure. The Sea Beam can be used for that purpose by introduction of a fictitious speed in order to keep the plot running even though the ship is not moving. Motion of the ship relative to the bottom can be monitored, and corrections applied. For extensive station work,

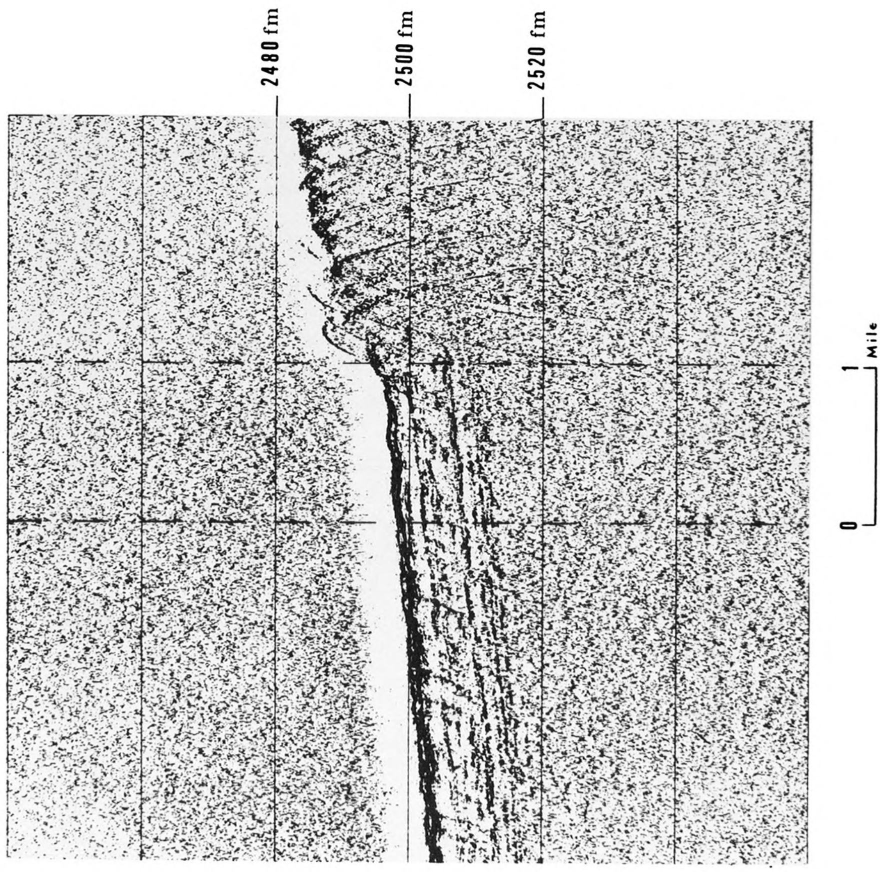

FIG. 28. — Mud penetrator (3.5 Kc) profile over lower continental slope between Test Areas 1 and 2 showing an abrupt change from stratified to deformed sediments around 4 700 meters (2 500 fathoms).

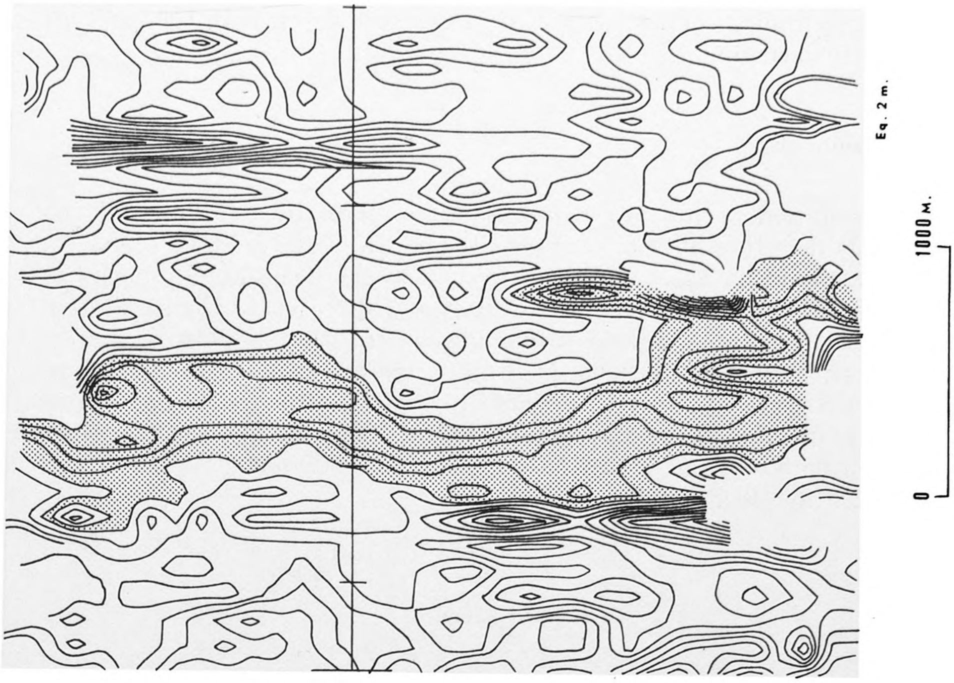

FIG. 29. — Sea Beam profile corresponding to fig. 28, contour interval 2 m, original scale 1/20 000, sea state 5.

multi-beam technology could be applied to measure depth both fore and aft as well as athwartship.

Limit of resolution

The resolution of the Sea Beam decreases with the obliquity of the beams and is therefore not uniform over the width of the contour plots. As seen earlier, the mean accuracy of the system in the deep ocean appears to be better than 10 meters after removal of systematic errors. Figure 28 is a 3.5 Kc record showing a change from a well stratified smooth area to a disturbed one with undulations of a few meters. The two zones are separated by a scarp of about 10 meters. Figure 29 is the Sea Beam record across that transition. The scarp is well outlined, but the change in bottom character on both sides of it can only be seen on the analog record of the vertical beam, due to its higher resolution.

CONCLUSION

In summary, the Sea Beam has turned out to be a perfectly operational system. On all points it has performed to our high expectations. The three dimensional vision that it gives of the ocean floor is such a major step forward that conventional mono-beam systems will soon become obsolete. First cruise results have confirmed the great advances that multi-beam sonars will trigger in the field of marine cartography and sea floor morphology. Real time merging of Sea Beam data with an integrated navigation system will further increase the potential of this new tool.

REFERENCES

[1] Sea-Beam for precise bathymetric surveys, Technical Bulletin, General Instrument Corporation, Harris ASW Division, Westwood, Massachusetts, 43 p., May 1977.

[2] Introducing an operational multi-beam array sonar. Morris F. GLENN. *Intern. Hydrog. Review*, Monaco, Vol. XLVII (1), Jan. 1970, pp. 35-39.

[3] Le Sea-Beam, sondeur multi-faisceaux du *Jean Charcot*. Notice technique par Jean-Paul ALLENOU et Vincent RENARD, Centre Océanologique de Bretagne, Rapport Scientifique et Technique, N° 37, 1978.

[4] ATNAV II, The Expanded Capacity Acoustic Transponder Navigation System, Technical Bulletin, AMF Sea-Link Systems, Herndon, Virginia, 19 p., April 1977.

[5] BO'SUN : A high resolution automatic charting system for continental shelf, Harold K. FARR. General Instrument Corporation, Harris ASW Division, Westwood, Mass., USA.

[6] An evaluation of the Bo'sun multi-beam sonar system. R. BURKE and J. ROBSON, *Intern. Hydrog. Review*, Monaco, LII (2), July 1975, pp. 53-69.

[7] Kriging : A method for cartography of the sea floor. J.P. CHILES, P. CHAUVET. *Intern. Hydrog. Review,* Vol. LII (1), Jan. 1975, pp. 25-41.

[8] Application du filtre de Kalman à la navigation. J.P. FAIL. *Geophys. Prospecting,* Vol. 20, pp. 665-699, 1972.

[9] Integrated navigation systems for precise positioning in the deep ocean. K. KASMEYER, *Marine Geodesy,* Vol. 1, No. 1, 1977.

[10] Bathymétrie détaillée d'une vallée du Rift et de faille transformante, effectuée dans le cadre du projet FAMOUS, par V. RENARD, B. SCHRUMPF et J.C. SIBUET, Centre Océanologique, Brest, 1975.

[11] Relevé du canyon sous-marin de Guilvinec avec le sondeur Sea-Beam, marge continentale armoricaine, par Vincent RENARD *et al,* Centre Océanologique de Bretagne. In preparation.